RSC Advances

PAPER

View Article Online
View Journal | View Issue

Cite this: *RSC Adv.*, 2015, **5**, 98527

Synthesis, biological evaluation and mechanism study of a class of cyclic combretastatin A-4 analogues as novel antitumour agents†

Jun Yan, Yanqing Pang, Jie Chen, Jianfei Sheng, Jinhui Hu, Ling Huang* and Xingshu Li*

Received 18th September 2015
Accepted 3rd November 2015

DOI: 10.1039/c5ra19270f

www.rsc.org/advances

In the course of our search for novel antitumor agents, a series of cyclic combretastatin A-4 (**CA-4**) analogues bearing an amide group, A–B or B–C ring condensation, and C=C or C=N bond in the B ring were designed, synthesized and identified as new microtubule inhibitors. The structure–activity relationship (SAR) studies showed that the hexa-cyclic compounds bearing B–C ring condensation, containing a C=C bond in the B ring (**4a**) provided excellent antiproliferative activities at nanomolar concentrations against various cancer cell lines (IC_{50} = 46–80 nM). **4a** inhibited tubulin assembly at a micromolar range (IC_{50} = 2.56 ± 0.15 μM) as evidenced by a molecular docking study, which revealed that **4a** exerted tubulin polymerisation inhibitory activity by binding to the colchicine binding site of tubulin. Further molecular biology studies showed that **4a** disrupted intracellular microtubule polymerisation and thus induced G2/M phase arrest and apoptotsis in A549 cells. Altogether, these results we obtained can guide the design of novel potent molecules for future development.

Introduction

The tubulin–microtubule system, which is crucially involved in cell mitosis, is an attractive target for the development of highly efficient anticancer drugs.[1–3] Among them, combretastatin A-4 (**CA-4**, Fig. 1), first isolated from the bark of the African willow tree in 1982,[4] dramatically disrupts tubulin assembly and its disodium phosphate (**CA-4P**) has been approved for clinical trials.[5–7] However, the *cis*-stilbene structure in **CA-4** is prone to isomerize to the more thermodynamically stable, but less bioactive *trans* isomers.[8,9] To overcome this shortcoming, lots of modifications to stabilize the conformation by replacement of the olefinic bridge with a ring or carbonyl have been developed in recent decades.[10–14]

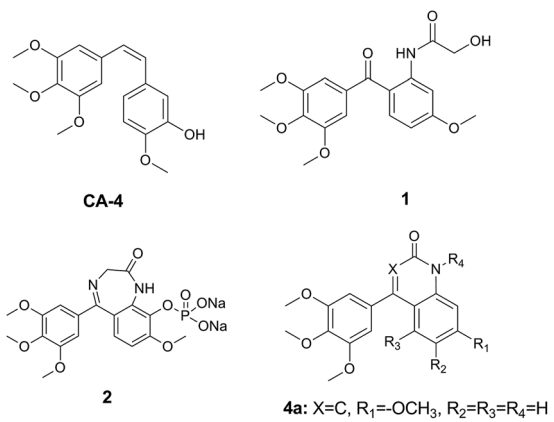

Fig. 1 Design strategy for combretastatin A-4 analogues.

In our previous work,[15,16] *via* a simple cross-coupling strategy in aqueous solution with polyethylene glycol as additive under very mild conditions, we have synthesized and evaluated a new series of *ortho*-(3,4,5-trimethoxybenzoyl)-acetanilides as tubulin polymerisation inhibitors. Among them, compound **1** (Fig. 1) exhibited excellent anti-proliferative activity against various human cancer cell lines.[16] Subsequently, on reaction of the *ortho*-(3,4,5-trimethoxybenzoyl)-bromoacetanilides with NH_3 in water, we obtained a series of cyclic compounds including compound **2** (Fig. 1) which displayed excellent anti-tumour activity *in vitro* and *in vivo*.[17] To investigate the detailed structure and activity relationships (SARs), we designed and synthesized another seventeen cyclic **CA-4** analogues, and mainly focused on three aspects: the number of atoms in the B ring (hexa-cyclic or hepta-cyclic compounds), the pattern of ring condensation (A–B ring condensation or B–C ring condensation), and the effect of a C=C or C=N bond in the B ring. In addition to the synthesis work, we evaluated the anti-proliferative activities of all the synthesized compounds toward different types of cancer cells, and also investigated the mechanism of their anti-proliferative activity.

School of Pharmaceutical Sciences, Sun Yat-sen University, Guangzhou, 510006, China. E-mail: huangl72@mail.sysu.edu.cn; lixsh@mail.sysu.edu.cn

† Electronic supplementary information (ESI) available. See DOI: 10.1039/c5ra19270f

Results and discussion

Chemistry

Compounds **4a–d**, **5**, **9**, and **12** were synthesized using the route in Scheme 1. First, according to the previous method, key intermediates **3a–d**, **8**, and **11** were conveniently obtained by the reaction of acetanilides with 3,4,5-trimethoxybenzaldehyde in the presence of 5% $Pd(OAc)_2$ and polyethylene glycol as the additive. The intermolecular aldol condensation was performed in the presence of CH_3ONa to afford cyclic compounds **4a–d**, **9**, and **12**. Then compound **4a** was reacted with methyl iodine to give **5**.

The reaction of 3-methoxaniline with benzyl chloroformate provided intermediate **13**. By the carbon–carbon cross-coupling reaction described above, compound **14** was obtained, which was de-protected and then reacted with urea at a temperature of 110 °C for 20 h to give compound **16** (Scheme 2).

Compounds **20a–e** were obtained with 2,3,4-trimethoxyaniline as starting material, by the same procedure of carbon–carbon cross coupling and intermolecular aldol condensation as above (Scheme 3).

Finally, the cross coupling reaction of compound **21**, which came from 2,3,4-trimethoxyaniline, with different aldehydes gave ketone derivatives **22a–d**. Compounds **22a–d** *via* ammonolysis and cyclization provided target compounds **23a–d** fluently (Scheme 4).

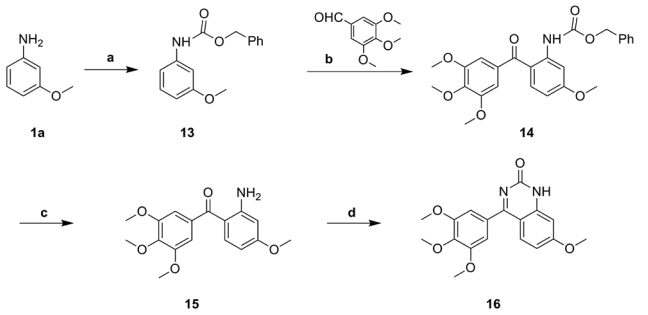

Scheme 2 Synthesis of compound **16**. Reagents and conditions: (a) benzyl chloroformate, Et_3N, CH_2Cl_2, rt, 1 h; (b) 5 mol% $Pd(OAc)_2$, 4 eq. TBHP, 26 mol% TFA, PEG-2000, water, rt, 12 h; (c) Pd/C, H_2, THF, rt, 4 h; (d) NH_2CONH_2, AcOH, 110 °C, 20 h.

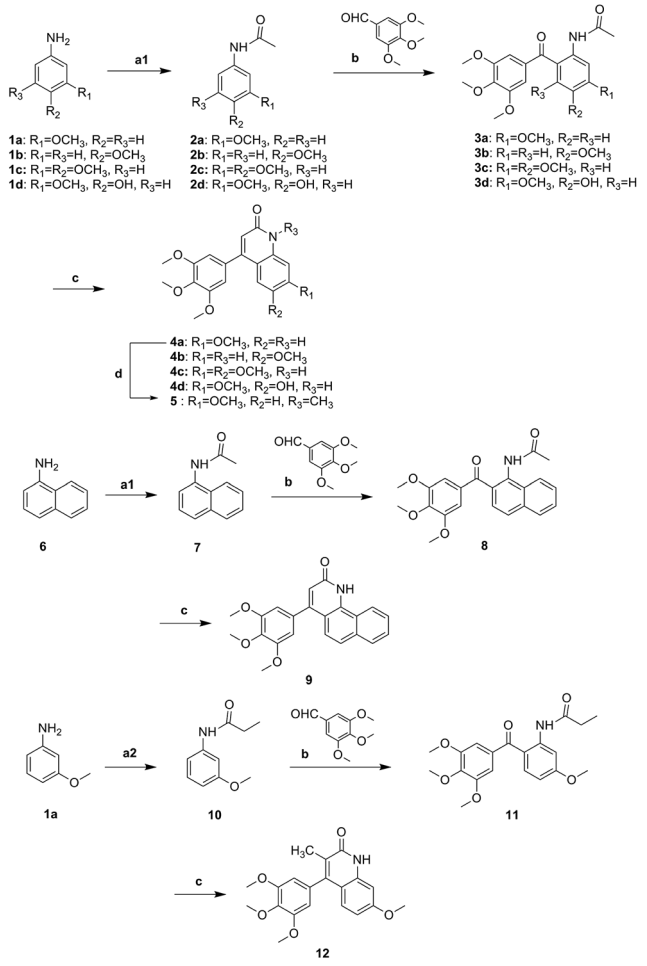

Scheme 1 Synthesis of compounds **4a–d**, **5**, **9**, and **12**. Reagents and conditions: (a_1) CH_3COCl, CH_2Cl_2, rt, 1 h; (a_2) CH_3CH_2COCl, CH_2Cl_2, rt, 1 h; (b) 5 mol% $Pd(OAc)_2$, 4 eq. TBHP, 26 mol% TFA, PEG-2000, water, rt, 12 h; (c) 10 eq. CH_3ONa, DMF, 90 °C, 12 h; (d) CH_3I, THF, rt, 12 h.

Biological evaluation

***In vitro* anti-proliferative activity.** To evaluate the anti-proliferative activities of the synthesized cyclic compounds, six human cancer cell lines, A549 (non-small-cell-lung cancer cell line), Bel-7402 (human liver carcinoma cell line), Hela (human epithelial cervical cancer cell line), MCF-7 (human breast carcinoma cell line), SW480 (human colon carcinoma cell line), and MGC-803 (human gastric cancer cell line) were tested using MTT (3-(4,5-dimethylthiazol-2-yl)-2,5-diphenyltetrazolium bromide) assay with **CA-4** as reference. The results shown in Tables 1–3 demonstrate that most of this series of compounds displayed good anti-proliferative activities

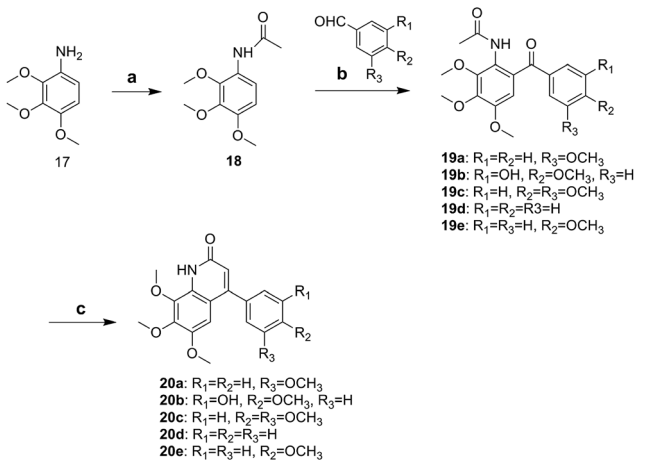

Scheme 3 Synthesis of compounds **20a–e**. Reagents and conditions: (a) CH_3COCl, CH_2Cl_2, rt, 1 h; (b) 5 mol% $Pd(OAc)_2$, 4 eq. TBHP, 26 mol% TFA, PEG-2000, water, rt, 12 h; (c) 10 eq. CH_3ONa, DMF, 90 °C, 12 h.

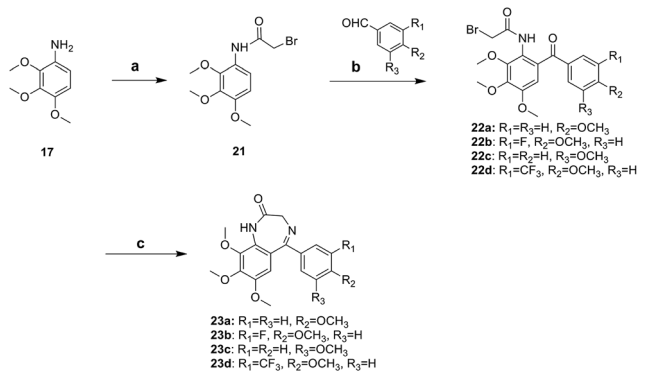

Scheme 4 Synthesis of compounds **23a–d**. Reagents and conditions: (a) $BrCH_2COCH_2Br$, CH_2Cl_2, rt, 1 h; (b) 5 mol% $Pd(OAc)_2$, 4 eq. TBHP, 26 mol% TFA, PEG-2000, water, rt, 12 h; (c) NH_3–H_2O, EtOH, rt, 6 h, reflux, 2 h.

with IC_{50} values in the micromolar to sub-micromolar range. It can be seen from Table 1, that compound **4a**, with three methoxyl groups on the A ring and one methoxyl on the C ring at the R_1 position, exhibited the best anti-proliferative activity towards all six cancer cell lines (IC_{50} = 0.046 μM for Hela, 0.074 μM for Bel-7402, 0.072 μM for A549, 0.08 μM for MCF-7, 0.074 μM for MGC-803 and 0.069 μM for SW480). Compounds **4b** and **4c**, with a methoxyl group at the R_2 position, or two methoxyl groups at both the R_1 and R_2 position, gave relatively poor activities (**4b** provided IC_{50} values in the range 0.33 to 1.20 μM, **4c** gave IC_{50} values in the range 0.80 to 4.45 μM). The replacement of the methoxyl group with a hydroxyl group at the R_2 position led to an almost complete loss of activity (**4d**, gave an IC_{50} value of more than 10 μM). An N-substituent in the B ring seems slightly unfavourable for the activity, compound **5** with CH_3 instead of H at R_3 position of **4a**, provided 0.52–1.14 μM IC_{50} values towards the six kinds of cancer cell lines. Compound **9**, where the benzene ring of **4** was replaced with a naphthalene ring gave almost 10-fold lower anti-proliferative activity compared with compound **4a**. When introducing a methyl group on the double bond of the B ring, we obtained compound **12**, which caused a nearly 20.4–110.9 fold decrease in anti-proliferative activity.

Besides the C=N double bond in the B ring, compound **16** has a very similar structure to compound **4a**. Unfortunately, surprisingly **16** exhibited poor activity toward all the six cancer cell lines (IC_{50} = 1.24 μM for Hela, and 7.98–12.1 μM for other cancer cell lines). These results showed that the C=C bond in B ring was very crucial for the anti-proliferative activity in this series compounds.

Compounds **20a–e**, with the characteristic of A–B ring condensation, were also evaluated for their anti-proliferative activities (Table 2). Compound **20a**, which has a similar structure to **4a** (besides B–C ring condensation in **4a**), provided activities that range from 1.05 μM to 5.82 μM, which were much lower than for its isomer **4a**. Compound **20b**, which has a hydroxyl in the R_1 position, gave the best result with IC_{50} values in a range from 0.204–0.968 μM. Other compounds, without a methoxyl group in the C ring (**20d**), or bearing a methoxyl group in the R_3 position (**20e**), or two methoxyl groups in the R_2 and R_3 position (**20c**), exhibited poor anti-proliferative activities. When compared to compound **4a**, compound **20a** showed a 14.2–87.4 fold decrease towards the six cancer cell lines, which demonstrated that A–B ring condensation is not favorable for the hexa-cyclic compounds.

Table 1 Anti-proliferative activities of compound **4a–d**, **5a**, **5b**, **9**, **12**, and **16** against different human cancer cell lines

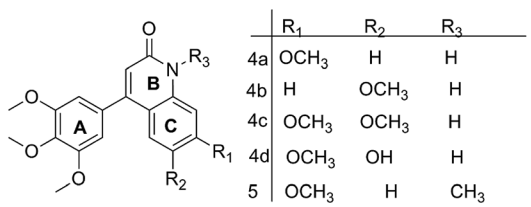

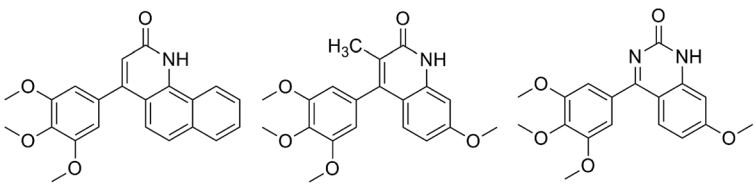

Compd.	IC_{50},[a] mean ± SE (μM)					
	Hela	Bel-7402	A549	MCF-7	MGC-803	SW480
4a	0.046 ± 0.01	0.074 ± 0.06	0.072 ± 0.009	0.08 ± 0.009	0.074 ± 0.19	0.069 ± 0.03
4b	0.47 ± 0.11	0.79 ± 0.02	0.817 ± 0.04	0.637 ± 0.287	0.33 ± 0.06	1.20 ± 0.25
4c	0.99 ± 0.17	1.48 ± 0.67	0.80 ± 0.14	1.67 ± 0.83	4.45 ± 0.02	3.69 ± 0.25
4d	>10	>10	>10	>10	>10	>10
5	0.67 ± 0.08	0.59 ± 0.05	0.52 ± 0.04	0.74 ± 0.02	0.72 ± 0.25	1.14 ± 0.01
9	0.34 ± 0.006	1.95 ± 0.52	2.56 ± 0.08	3.395 ± 0.658	5.20 ± 0.91	7.60 ± 0.85
12	0.94 ± 0.20	1.30 ± 0.30	1.72 ± 0.44	6.16 ± 2.05	1.92 ± 0.32	7.65 ± 0.19
16	1.24 ± 0.05	8.22 ± 0.03	8.74 ± 0.31	7.98 ± 0.06	11.0 ± 0.14	12.1 ± 0.15
CA-4	0.003 ± 0.002	0.012 ± 0.001	0.005 ± 0.001	0.013 ± 0.001	0.009 ± 0.002	0.0017 ± 0.002

[a] Data are presented as the mean ± SE from the dose–response curves of at least three independent experiments.

Table 2 Anti-proliferative activities of compound **20a–e** against different human cancer cell lines

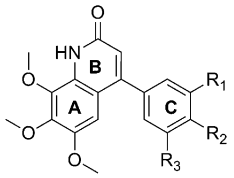

	R_1	R_2	R_3
20a	H	OCH_3	H
20b	OH	OCH_3	H
20c	H	OCH_3	OCH_3
20d	H	H	H
20e	H	H	OCH_3

	IC_{50},[a] mean ± SE (μM)					
Compd.	Hela	Bel-7402	A549	MCF-7	MGC-803	SW480
20a	4.02 ± 0.46	1.05 ± 0.08	4.82 ± 0.09	3.69 ± 0.19	5.82 ± 0.13	1.16 ± 0.03
20b	0.204 ± 0.03	0.789 ± 0.13	0.307 ± 0.06	0.487 ± 0.35	0.968 ± 0.29	0.892 ± 0.06
20c	15.8 ± 0.23	20.6 ± 0.26	18.6 ± 0.69	19.6 ± 0.28	18.4 ± 0.17	18.6 ± 0.24
20d	25.1 ± 0.56	28.6 ± 0.17	37.6 ± 0.84	31.2 ± 0.14	30.6 ± 0.15	24.9 ± 0.07
20e	10.4 ± 0.25	10.6 ± 0.31	15.6 ± 0.59	11.2 ± 0.19	14.6 ± 0.21	9.84 ± 0.28
CA-4	0.005 ± 0.001	0.012 ± 0.001	0.003 ± 0.002	0.013 ± 0.001	0.009 ± 0.002	0.0017 ± 0.002

[a] Data are presented as the mean ± SE from the dose–response curves of at least three independent experiments.

To further examine the relationship between the structure and the anti-proliferative activity of cyclic-**CA-4** analogues, **23a–e** (A–B ring condensation) were synthesized and tested against the different cancer cell lines. As shown in Table 3, compounds **23a–e** exhibited good activities against the six cancer cell lines. When compared to **20a**, compound **23a** showed an almost 16.8-fold increase of antiproliferative activity toward Hela cell lines, which indicated that the hepta-ring was more favourable for the activity than the hexa-ring.

***In vitro* inhibition of tubulin polymerisation.** To study whether these compounds target the tubulin–microtubule system, compounds **4a**, **20b**, **23a**, and **23b**, which showed relatively better anti-proliferative activity *in vitro*, were chosen to investigate their ability to block microtubule assembly by the method originally described by Bonne, D. *et al.* with moderate modification,[17,18] with **CA-4** as the reference compound. The results summarized in Table 4 show that compound **4a**, which gave the best anti-proliferative activity *in vitro*, also displayed the most potent inhibitory activity on tubulin polymerisation, with an IC_{50} of 2.56 μM. Compounds **20b**, **23a**, and **23b**, with lower anti-proliferative activity, provided slightly reduced inhibitory activity toward tubulin polymerisation accordingly. The correlation between the anti-proliferative activity and the tubulin polymerisation inhibitory activity indicated that the synthesized compounds indeed target the tubulin–microtubule system, which was consistent with most antimitotic agents.[19]

It is well known that tubulin-binding agents can be broadly classified into two types: stabilizing agents (such as taxanes) and destabilizing agents (such as colchicine and **CA-4**).[14,20] To confirm which type compound **4a** belongs to, we carried out

Table 3 Anti-proliferative activities of compound **23a–e** against different human cancer cell lines

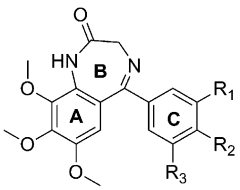

	R_1	R_2	R_3
23a	H	OCH_3	H
23b	F	OCH_3	H
23c	H	H	OCH_3
23d	CF_3	OCH_3	H

	IC_{50},[a] mean ± SE (μM)					
Compd.	Hela	Bel-7402	A549	MCF-7	MGC-803	SW480
23a	0.24 ± 0.17	0.282 ± 0.06	0.306 ± 0.03	0.261 ± 0.21	0.381 ± 0.28	0.493 ± 0.29
23b	0.21 ± 0.27	0.184 ± 0.01	0.175 ± 0.32	0.31 ± 0.15	0.58 ± 0.18	0.384 ± 0.01
23c	3.95 ± 0.22	5.69 ± 0.05	4.304 ± 0.71	4.05 ± 0.07	5.94 ± 0.13	3.87 ± 0.21
23d	5.64 ± 0.25	4.16 ± 0.31	7.62 ± 0.59	3.27 ± 0.19	4.62 ± 0.21	3.84 ± 0.28
CA-4	0.005 ± 0.001	0.012 ± 0.001	0.003 ± 0.002	0.013 ± 0.001	0.009 ± 0.002	0.0017 ± 0.002

[a] Data are presented as the mean ± SE from the dose–response curves of at least three independent experiments.

Table 4 The IC_{50} values of selected compounds on inhibition of tubulin polymerisation

Compd.	4a	20b	23a	23b	CA-4
IC_{50},[a]mean± SE (μM)	2.56 ± 0.15	4.15 ± 0.21	3.34 ± 0.35	3.01 ± 0.03	1.20 ± 0.04

[a] Data are presented as the mean ± SE from the dose–response curves of at least three independent experiments.

microtubule dynamics assays with 0.938, 1.875, 3.75, 7.5, and 15 μM of compound **4a**, respectively. The representative raw data for the polymerisation assay of compound **4a** are shown in Fig. 2. As shown in Fig. 2, compound **4a** inhibited tubulin polymerisation in a concentration dependent manner, and thus is a microtubule destabilizing agent.

Disruption of microtubule dynamics. Given the important function of the tubulin–microtubule system in maintaining the cellular morphology,[1,12] immunofluorescence assays were performed to reveal whether compound **4a** could affect microtubule dynamics in living cells. Confocal microscopy studies clearly showed heavy disruption of the microtubule system of Hela cells after treatment with **4a**. As shown in Fig. 3, in the vehicle-treated group, microtubules were observed under the normal state, as evidenced by the regular assembly, slim, fibrous microtubules (green) wrapped around the cell nucleus (blue). While as the concentration of compound **4a** increased, the network of microtubules became disorganized and nuclear chromatin condensation appeared at a concentration of 100 nM. Furthermore, when the concentration increased to 200 nM, the spindle microtubules strikingly shrink around the centre of the cells, and the tubulin–microtubule system was heavily disrupted. These morphology changes of the microtubules implied that compound **4a** could easily interfere with the microtubule dynamics eventually leading to cell death.

Molecular docking study of 4a. As can be seen from the above results **4a** effectively inhibited the tubulin polymerisation *in vitro* and dramatically disrupted intracellular tubulin–microtubule dynamics. Then we performed a molecular docking study to elucidate the potential pose of compound **4a** to the colchicine binding site of α,β-tubulin. The MOE package was employed to investigate the docking between compound **4a** and α,β-tubulin. As shown in Fig. 4a, when we re-docked colchicine back to the colchicine binding site, the similar conformation of the X-ray structure of the colchicine (PDB code: 1SA0) verifies the reliability of our docking method. Then we employed this docking model for the docking of compound **4a**. The docking studies in Fig. 4B showed that **4a** occupied the colchicine binding site of tubulin, as evidenced by two hydrogen bonds and two σ–π conjugate actions were formed between **4a** and the residues of tubulin. The trimethoxyphenyl moiety of compound **4a** was positioned in the binding cavity buried in the β-subunit and formed a hydrogen bond with the thiol group of Cysβ241, and two key amino acids of β-tubulin (Leuβ248 and Leuβ255) formed hydrophobic interactions (σ–π conjugate) with the trimethoxyphenyl moiety. Overall, the *in silico* results correlate well with the tubulin polymerisation inhibition activity.

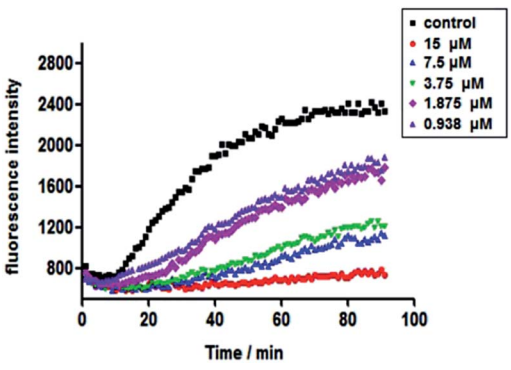

Fig. 2 The effect of compound **4a** on microtubule dynamics. Tubulin was mixed with the compound at different concentrations in general tubulin buffer containing 1 mM GTP and 20% glycerol. Microtubule polymerisation was monitored using the kinetic model of FlexStation 3 multimode reader (excitation, 360 nm; emission, 450 nm).

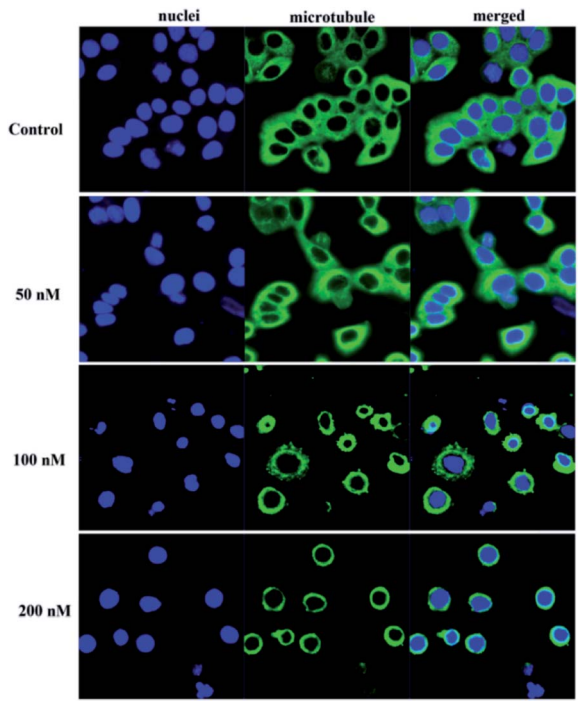

Fig. 3 Effects of **4a** on the cellular microtubule dynamics by immunofluorescence. Hela cells were incubated with 0.1% DMSO or 50, 100, and 200 nM compound **4a** at 37 °C for 24 h, and then direct microscopy detection of the fixed and stained cells was performed. Images were taken using an LSM 570 laser confocal microscope (Carl Zeiss, Germany). The experiments were performed three times, and the results of representative experiments are shown.

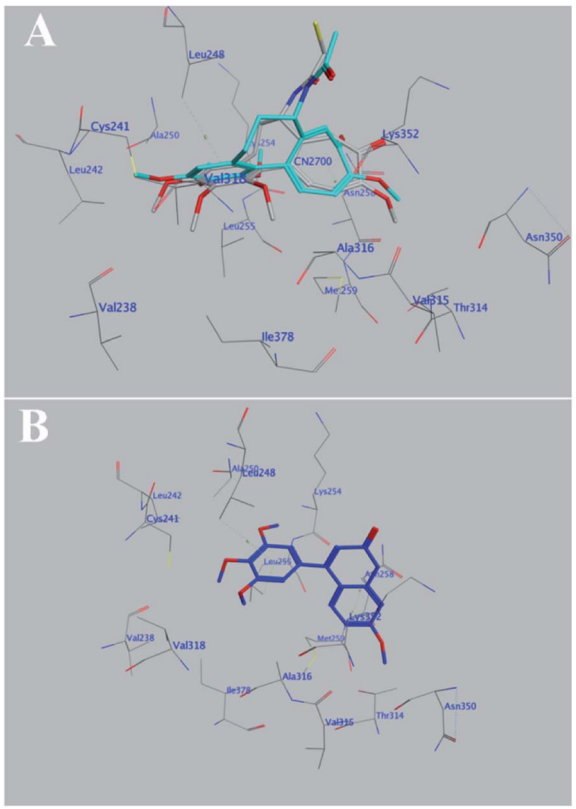

Fig. 4 Proposed binding mode for compounds colchicine (A) and **4a** (B), obtained by molecular docking simulation into the colchicine binding pocket of β-tubulin.

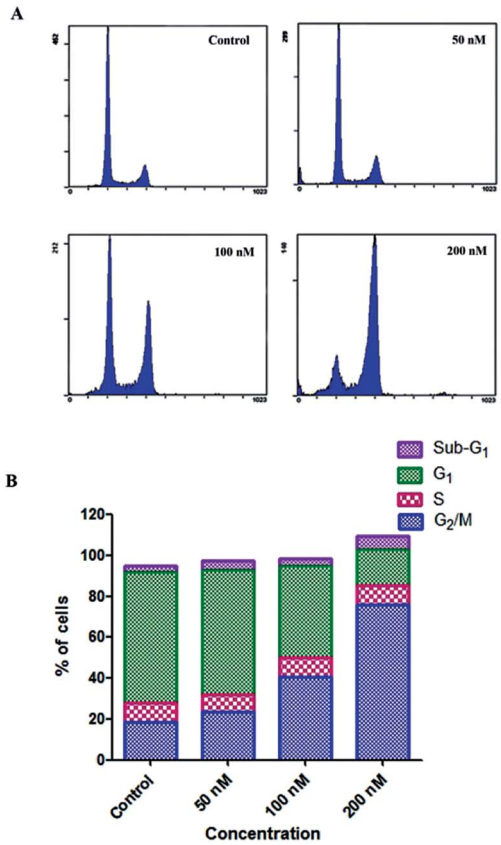

Fig. 5 Cell cycle distribution of Hela cells with compound **4a**. Cells were treated with compound **4a** (50, 100, and 200 nM) or DMSO (0.01%) for 48 h. The DNA contents of each cell phase were analyzed by flow cytometry (A) quantitative analysis of the percentage of cells in each cell cycle phase was analysed by EXPO32 ADC analysis software (B). The experiments were performed three times, and the results of representative experiments are shown.

Cell cycle arrest at the G_2/M phase. It is well known that most tubulin polymerisation inhibition agents induce cytoskeleton disruption and then block the cell cycle in the G_2/M phase.[21] The excellent potency of compound **4a** on tubulin polymerisation inhibition prompted us to evaluate its effects on the cell cycle. After Hela cells were treated with compound **4a** at different concentrations (50, 100, and 200 nM) and DMSO (0.01%) as the reference for 48 h, an analysis of the results of harvested cells by flow cytometry indicated that **4a** resulted in a significant cell-cycle arrest at the G_2/M phase, and showed a dose-dependent manner (Fig. 5). As shown in Fig. 5, the control group showed 18.3% of the cells at the G_2/M phase. Whereas, when the cells were treated with **4a** at 50, 100, and 200 nM, the cells at the G_2/M phase correspondingly increased to 23.5%, 40.7% and 75.9%, respectively. Furthermore, as the concentration of compound **4a** was increased, a typical apoptosis sub-peak was also obviously observed in the DNA histogram (Fig. 5A), which revealed that compound **4a** might have the ability to induce cell apoptosis. Therefore, we concluded that compound **4a** could arrest cell-cycle progression at the mitotic phase, which is in agreement with most of the antimitotic agents.

Compound 4a induces apoptosis of Hela cells. As an obvious typical apoptosis sub-peak appeared in the cell cycle analysis (Fig. 5A), we hypothesized that compound **4a** might induce cell apoptosis. To confirm this property, compound **4a** treated Hela cells were stained with Annexin V-FITC and PI, and analyzed by flow cytometry. The data summarized in Fig. 6 show that **4a** induced cell apoptosis in a dose-dependent manner. The total percentage of early and late apoptotic cells were 2.21%, 23.40%, and 40.90% in the cases of 50, 100, and 200 nM **4a** treated Hela cells, respectively. In contrast, the apoptotic cells were almost negligible in the control group, which revealed that compound **4a** could exclusively trigger apoptotic cell death of the Hela cells. These results further demonstrated that the anti-proliferative activity of compound **4a** was due to its interaction with tubulin, resulting in a prolonged cell cycle arrest that eventually leads to cell apoptosis.

Metabolic stability. As well discussed in previous literature, the *cis* double bond in **CA-4** is prone to isomerize to the more thermodynamically stable, but less bioactive *trans* isomers.[8,9] To evaluate the stability of the synthesized cyclic **CA-4** analogues, the optimal compound **4a** and the reference compound **CA-4** were investigated for their metabolic stability in rat liver microsomes. When incubated in the presence of rat liver microsomes (Table 5), **CA-4** displayed a relatively fast metabolic profile, with substrate remaining ranging from 68.1% to 20.7% after 30 to 120 min. Under the same conditions, **4a** exhibited

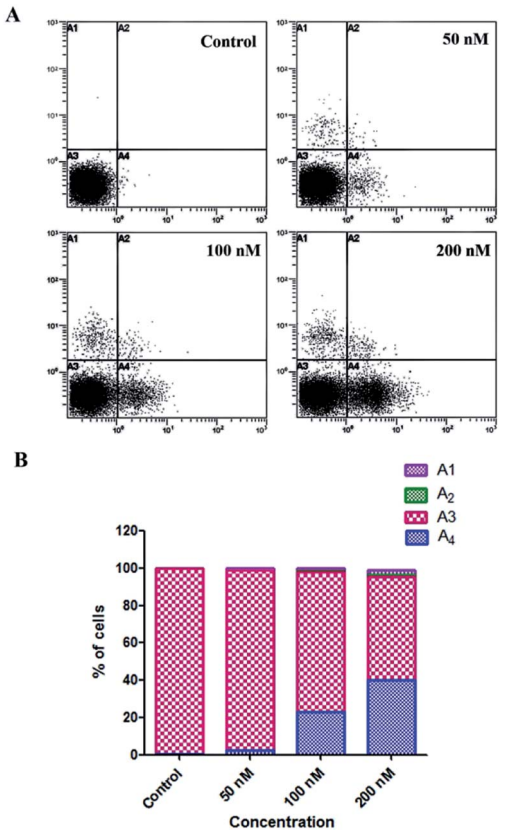

Fig. 6 Compound **4a** induced apoptosis of Hela cells. Cells were treated with compound **4a** (50, 100, and 200 nM) or DMSO (0.01%) for 48 h. Then the cells were collected and analyzed by flow cytometry after being stained by Annexin V-FITC and PI (A). The percentages of cells in each stage of cell apoptosis were quantitated by flow cytometry. (A1: upper left quadrant) necrotic cells; (A2: upper right quadrant) late apoptotic cells; (A3: bottom left quadrant) live cells; and (A4: bottom right quadrant) early apoptotic cells (B). The experiments were performed three times, and representative experiments are shown.

Table 5 The metabolic stability of **4a** and **CA-4**

	Substrate remaining			
	Time/min			
	30	60	90	120
4a	69.6%	49.2%	42.9%	36.5%
CA-4	68.1%	28.6%	23.1%	20.7%

69.6–36.5%, which indicated that **4a** has relatively better metabolic stability than **CA-4.**

Experimental section

Chemistry

General methods. All reagents used in the synthesis were obtained commercially and used without further purification, unless otherwise specified. The ^{1}H NMR and ^{13}C NMR spectra were recorded using TMS as the internal standard on a Bruker BioSpin GmbH spectrometer at 400 and 101 MHz, respectively. High-resolution mass spectra (HR-MS) were recorded using a Shimadzu LCMS-ITTOF mass spectrometer. The melting points were determined using an SRS-OptiMelt automated melting point instrument. The reactions were monitored by thin layer chromatography (TLC) on glass-packed percolated silica gel plates and visualized in an iodine chamber or with a UV lamp. Flash column chromatography was performed using silica gel (200–300 mesh) purchased from Qingdao Haiyang Chemical Co. Ltd. The purity (≥95%) of the synthesised compounds was determined by high-performance liquid chromatography (HPLC) with a TC-C18 column (4.6 × 250 mm, 5 μm), an acetonitrile–water or methanol–water mobile phase, and a flow rate of 1.00 mL min^{-1}.

General procedure for the preparation of substituted acetanilide substrates (2a–d, 7, 10, 21).[22,23] All the substituted anilides were prepared from the corresponding anilines and acyl chlorides in CH_2Cl_2 according to the literature method without modifications.

General procedure for the coupling reactions.[15,16,24,25] Substituted anilide, 3,4,5-trimethoxybenzaldehyde (2.0 equiv.), $Pd(OAc)_2$ (0.05 equiv.) and PEG-2000 (0.2 equiv.) were loaded into a Schlenk tube, and then water was added to the mixture. After stirring for 2 min, TBHP (4.0 equiv.) and trifluoroacetic acid (0.26 equiv.) were added to the mixture at room temperature. The mixture was stirred at 40 °C for 12 hours and then cooled to room temperature. A saturated solution of K_2CO_3 was added and the mixture was extracted with ethyl acetate. The combined organic phase was washed (brine) and concentrated under reduced pressure to give the crude products which were purified by flash column chromatography on silica gel (200–300 mesh) to afford the desired product.

General procedure for the synthesis of 4a–d, 9, 12, 20a–e. To a stirred solution of intermediates **3a–d**, **8**, **11** and **19a–e** in anhydrous DMF, CH_3ONa (10.0 equiv.) was added. After refluxing for 12 h, the solvents were evaporated under vacuum, and the residue was extracted with CH_2Cl_2, washed (brine), dried (Na_2SO_4), filtered and concentrated under vacuum to provide the crude product, which was purified by column chromatography to afford a white solid.

7-Methoxy-4-(3,4,5-trimethoxyphenyl)quinolin-2(1H)-one ***(4a).*** Yellow solid; yield 52.2%; mp: 261.9–262.6 °C; ^{1}H NMR (400 MHz, $CDCl_3$) δ 11.99 (s, 1H), 7.54 (d, J = 9.0 Hz, 1H), 6.89 (d, J = 2.4 Hz, 1H), 6.79 (dd, J = 9.0, 2.4 Hz, 1H), 6.67 (s, 2H), 6.54 (s, 1H), 3.94 (s, 3H), 3.93 (s, 3H), 3.88 (d, J = 7.0 Hz, 6H).^{13}C NMR (101 MHz, $CDCl_3$) δ 164.61, 161.93, 153.40, 153.31, 140.87, 138.44, 132.93, 128.08, 117.38, 113.73, 112.35, 106.13, 98.69, 60.97, 56.28, 55.73. HRMS (ESI) (m/z) $[M + H]^+$ calcd for $C_{19}H_{19}NO_5$, 342.1336; found, 342.1340. Purity: 99.7% (by HPLC).

6-Methoxy-4-(3,4,5-trimethoxyphenyl)quinolin-2(1H)-one ***(4b).*** White solid; yield 61%; mp: 283.0–283.5 °C; ^{1}H NMR (400 MHz, $CDCl_3$) δ 12.64 (s, 1H), 7.48 (d, J = 8.9 Hz, 1H), 7.20 (dd, J = 8.9, 2.6 Hz, 1H), 7.11 (d, J = 2.6 Hz, 1H), 6.72 (d, J = 6.8 Hz, 3H), 3.95 (d, J = 8.3 Hz, 3H), 3.90 (s, 6H), 3.76 (s, 3H).^{13}C NMR (101 MHz, $CDCl_3$) δ 163.83, 155.17, 153.40, 152.78, 138.44, 133.63, 132.67, 120.92, 120.11, 120.02, 118.07, 108.26, 106.03, 61.00, 56.28,

55.67. HRMS (ESI) (*m*/*z*) $[M + H]^+$ calcd for $C_{19}H_{19}NO_5$, 342.1336; found, 342.1327. Purity: 99.9% (by HPLC).

*6,7-Dimethoxy-4-(3,4,5-trimethoxyphenyl)quinolin-2(1H)-one (**4c**).* White solid; yield 58%; mp: 226.3–227.0 °C; ^{1}H NMR (400 MHz, $CDCl_3$) δ 12.77 (s, 1H), 7.06 (s, 1H), 6.98 (s, 1H), 6.71 (s, 2H), 6.60 (s, 1H), 4.04 (s, 3H), 3.96 (s, 3H), 3.90 (s, 6H), 3.79 (s, 3H).^{13}C NMR (101 MHz, $CDCl_3$) δ 164.32, 153.39, 152.86, 152.79, 145.80, 138.40, 135.11, 133.08, 117.62, 112.76, 107.00, 105.99, 98.67, 60.99, 56.40, 56.28, 56.15. HRMS (ESI) (*m*/*z*) $[M + H]^+$ calcd for $C_{20}H_{21}NO_6$, 372.1442; found, 372.1439. Purity: 99.8% (by HPLC).

*6-Hydroxy-7-methoxy-4-(3,4,5-trimethoxyphenyl)quinolin-2(1H)-one (**4d**).* White solid; yield 51%; mp: 184.5–187.6 °C; ^{1}H NMR (400 MHz, DMSO) δ 11.72 (s, 1H), 6.98 (s, 1H), 6.94 (s, 1H), 6.73 (s, 2H), 6.29 (s, 1H), 3.83 (s, 9H), 3.74 (s, 3H).^{13}C NMR (101 MHz, DMSO) δ 161.41, 153.38, 152.18, 152.06, 143.43, 138.14, 134.11, 133.10, 117.07, 112.93, 110.42, 106.56, 98.80, 60.55, 56.52, 56.14. HRMS (ESI) (*m*/*z*) $[M + H]^+$ calcd for $C_{19}H_{19}NO_6$, 358.1285; found, 358.1279. Purity: 97.3% (by HPLC).

*4-(3,4,5-Trimethoxyphenyl)benzo[h]quinolin-2(1H)-one (**9**).* White solid; yield 56%; mp: 262.1–263.5 °C; ^{1}H NMR (400 MHz, $CDCl_3$) δ 12.01 (s, 1H), 8.81 (d, J = 8.5 Hz, 1H), 7.92 (d, J = 7.5 Hz, 1H), 7.79–7.74 (m, 1H), 7.69 (t, J = 7.2 Hz, 1H), 7.64 (d, J = 8.9 Hz, 1H), 7.58 (d, J = 8.9 Hz, 1H), 6.87 (s, 1H), 6.73 (s, 2H), 3.98 (s, 3H), 3.92 (s, 6H).^{13}C NMR (101 MHz, $CDCl_3$) δ 163.68, 154.17, 153.37, 138.38, 136.08, 134.10, 133.11, 128.58, 128.30, 127.19, 123.35, 122.91, 122.29, 121.81, 120.53, 115.67, 106.24, 61.04, 56.33. HRMS (ESI) (*m*/*z*) $[M + H]^+$ calcd for $C_{22}H_{19}NO_4$, 362.1387; found, 362.1371. Purity: 99.5% (by HPLC).

*7-Methoxy-3-methyl-4-(3,4,5-trimethoxyphenyl) quinolin-2(1H)-one (**12**).* White solid; yield 48%; mp: 294.2–294.8 °C; ^{1}H NMR (400 MHz, $CDCl_3$) δ 11.78 (s, 1H), 7.07 (d, J = 9.0 Hz, 1H), 6.87 (d, J = 2.4 Hz, 1H), 6.71 (dd, J = 9.0, 2.4 Hz, 1H), 6.44 (s, 2H), 3.95 (s, 3H), 3.90 (s, 3H), 3.86 (s, 6H), 2.08 (s, 3H).^{13}C NMR (101 MHz, $CDCl_3$) δ 164.78, 160.80, 153.49, 148.92, 138.60, 137.42, 132.70, 128.14, 124.16, 115.28, 111.58, 105.75, 98.21, 61.00, 56.22, 55.57, 14.01. HRMS (ESI) (*m*/*z*) $[M + H]^+$ calcd for $C_{20}H_{21}NO_5$, 356.1492; found, 356.1487. Purity: 99.1% (by HPLC).

*6,7,8-Trimethoxy-4-(4-methoxyphenyl)quinolin-2(1H)-one (**20a**).* Yellow solid; yield 61%; mp: 228.4.0–229.7 °C; ^{1}H NMR (400 MHz, $CDCl_3$) δ 9.16 (s, 1H), 7.04 (d, J = 1.6 Hz, 1H), 6.98 (d, J = 8.2 Hz, 1H), 6.94 (dd, J = 8.2, 1.7 Hz, 1H), 6.82 (s, 1H), 6.53 (s, 1H), 5.96 (s, 1H), 4.04 (s, 3H), 3.98 (d, J = 4.1 Hz, 6H), 3.76 (s, 3H).^{13}C NMR (101 MHz, $CDCl_3$) δ 161.77, 159.77, 152.19, 149.06, 143.99, 139.22, 138.54, 129.74, 127.81, 120.94, 120.80, 114.90, 114.52, 114.15, 103.28, 61.44, 61.21, 56.22, 55.38. HRMS (ESI) (*m*/*z*) $[M + H]^+$ calcd for $C_{19}H_{19}NO_5$, 342.1336; found, 342.1321. Purity: 96.4% (by HPLC).

*4-(3-Hydroxy-4-methoxyphenyl)-6,7,8-trimethoxyquinolin-2(1H)-one (**20b**).* White solid; yield 51%; mp: 235.3.0–236.1 °C; ^{1}H NMR (400 MHz, $CDCl_3$) δ 9.16 (s, 1H), 7.42 (t, J = 7.9 Hz, 1H), 7.05–7.00 (m, 2H), 6.99–6.96 (m, 1H), 6.76 (s, 1H), 6.56 (s, 1H), 4.05 (s, 3H), 3.97 (s, 3H), 3.86 (s, 3H), 3.74 (s, 3H).^{13}C NMR (101 MHz, $CDCl_3$) δ 161.72, 152.14, 149.04, 147.22, 145.79, 143.86, 139.06, 130.37, 127.62, 120.55, 120.51, 115.09, 115.04, 110.81, 103.44, 61.39, 61.20, 56.25, 56.04. HRMS (ESI) (*m*/*z*) $[M + H]^+$ calcd for $C_{19}H_{19}NO_6$, 358.1285; found, 358.1277. Purity: 100% (by HPLC).

*4-(3,4-Dimethoxyphenyl)-6,7,8-trimethoxyquinolin-2(1H)-one (**20c**).* Yellow solid; yield 61%; mp: 221.0–222.4 °C; ^{1}H NMR (400 MHz, $CDCl_3$) δ 9.14 (s, 1H), 7.05–7.00 (m, 2H), 6.97 (d, J = 1.7 Hz, 1H), 6.82 (s, 1H), 6.56 (s, 1H), 4.05 (s, 3H), 3.98 (d, J = 2.1 Hz, 6H), 3.91 (s, 3H), 3.75 (s, 3H).^{13}C NMR (101 MHz, $CDCl_3$) δ 161.87, 152.06, 149.55, 148.98, 143.91, 139.28, 129.77, 127.87, 121.21, 120.63, 115.06, 111.87, 111.24, 103.23, 61.43, 61.20, 56.17, 56.03, 55.98. HRMS (ESI) (*m*/*z*) $[M + H]^+$ calcd for $C_{20}H_{21}NO_6$, 372.1442; found, 372.1434. Purity: 100% (by HPLC).

*6,7,8-Trimethoxy-4-phenylquinolin-2(1H)-one (**20d**).* Yellow solid; yield 68%; mp: 214.0–215.3 °C; ^{1}H NMR (400 MHz, $CDCl_3$) δ 9.15 (s, 1H), 7.51 (q, J = 5.2 Hz, 3H), 7.46–7.42 (m, 2H), 6.72 (s, 1H), 6.55 (s, 1H), 4.05 (s, 3H), 3.97 (s, 3H), 3.73 (s, 3H).^{13}C NMR (101 MHz, $CDCl_3$) δ 161.95, 152.27, 149.01, 144.02, 139.35, 137.25, 128.83, 128.67, 128.58, 127.95, 120.92, 114.98, 103.25, 61.45, 61.20, 56.16. HRMS (ESI) (*m*/*z*) $[M + H]^+$ calcd for $C_{18}H_{17}NO_4$, 312.1230; found, 312.1238. Purity: 99.3% (by HPLC).

*6,7,8-Trimethoxy-4-(3-methoxyphenyl)quinolin-2(1H)-one (**20e**).* Yellow solid; yield 60%; mp: 273.0–273.5 °C; ^{1}H NMR (400 MHz, $CDCl_3$) δ 9.10 (s, 1H), 7.39 (d, J = 8.6 Hz, 2H), 7.04 (d, J = 8.6 Hz, 2H), 6.78 (s, 1H), 6.53 (s, 1H), 4.05 (s, 3H), 3.97 (s, 3H), 3.90 (s, 3H), 3.75 (s, 3H).^{13}C NMR (101 MHz, $CDCl_3$) δ 161.85, 160.10, 152.04, 148.97, 143.89, 139.21, 129.91, 129.51, 127.82, 120.60, 115.15, 114.13, 103.33, 61.41, 61.20, 56.19, 55.37. HRMS (ESI) (*m*/*z*) $[M + H]^+$ calcd for $C_{19}H_{19}NO_5$, 342.1336; found, 342.1342. Purity: 100% (by HPLC).

*7-Methoxy-1-methyl-4-(3,4,5-trimethoxyphenyl)quinolin-2(1H)-one (**5**).* Compound **5** was synthesised following a previously reported procedure.[13] Briefly, to a solution of **4a** in anhydrous tetrahydrofuran, sodium hydride (2.0 equiv.) was added. After stirring for 30 min, CH_3I (1.5 equiv.) was added and then the mixture was stirred at room temperature for 12 h. The solvents were evaporated under vacuum, and the residue was extracted with CH_2Cl_2, washed with brine, dried over Na_2SO_4, filtered and concentrated under vacuum to give the crude product, which was purified by column chromatography to give a yellow solid. Yield 48%; mp: 179.1–180.2 °C; ^{1}H NMR (400 MHz, $CDCl_3$) δ 7.57 (d, J = 8.9 Hz, 1H), 6.87 (d, J = 2.3 Hz, 1H), 6.79 (dd, J = 8.9, 2.4 Hz, 1H), 6.63 (s, 2H), 6.55 (s, 1H), 3.93 (d, J = 1.8 Hz, 6H), 3.87 (s, 6H), 3.74 (s, 3H).^{13}C NMR (101 MHz, $CDCl_3$) δ 162.39, 161.77, 153.26, 150.81, 142.04, 138.30, 132.86, 129.14, 117.97, 114.52, 109.29, 106.18, 99.00, 60.95, 56.25, 55.60, 29.53. HRMS (ESI) (*m*/*z*) $[M + H]^+$ calcd for $C_{20}H_{21}NO_5$, 356.1492; found, 356.1497. Purity: 99.1% (by HPLC).

*(2-Amino-4-methoxyphenyl)(3,4,5-trimethoxyphenyl)methanone (**15**).* To a stirred suspension of benzyl 5-methoxy-2-(3,4,5-trimethoxybenzoyl)phenylcarbamate (**14**) in THF, 10% Pd/C was added and the mixture was hydrogenated in 30 Mpa of hydrogen pressure at room temperature for 4 h. The mixture was filtered and dried under vacuum to give the crude product, which was purified by column chromatography (petroleum ether–ethyl acetate) to give a yellow solid.

*7-Methoxy-4-(3,4,5-trimethoxyphenyl)quinazolin-2(1H)-one (**16**).* To a stirred suspension of compound **15** in acetic acid,

carbamide (2.0 equiv.) was added and then refluxed at 110 °C for 20 h. After the solvents were evaporated under vacuum, the mixture was extracted with ethyl acetate, washed with brine, dried over Na_2SO_4, filtered and concentrated under vacuum to give the crude product, which was purified by column chromatography to give a white solid. Yield 56%; mp: 254.9–255.8 °C; ^{1}H NMR (400 MHz, $CDCl_3$) δ 13.39 (s, 1H), 7.82 (d, J = 9.1 Hz, 1H), 7.00 (s, 2H), 6.96 (d, J = 2.3 Hz, 1H), 6.82 (dd, J = 9.1, 2.4 Hz, 1H), 3.96 (s, 3H), 3.95 (s, 3H), 3.93 (s, 6H).^{13}C NMR (101 MHz, $CDCl_3$) δ 175.12, 165.54, 158.89, 153.14, 146.31, 140.27, 132.16, 130.36, 114.32, 110.05, 107.20, 97.29, 61.00, 56.39, 56.23. HRMS (ESI) (m/z) [M + H]$^+$ calcd for $C_{18}H_{18}N_2O_5$, 343.1288; found, 343.1294. Purity: 98.5% (by HPLC).

General procedure for the synthesis of 23a–e. The intermediates **22a–e** were dissolved in ethanol, 25% ammonia solution was then added. After stirring at room temperature for 6 h, the reaction mixture was then refluxed for 2 h. The solvents were evaporated under vacuum to give the crude product, which was purified by column chromatography (petroleum ether–ethyl acetate, 1 : 1) to give the product.

*7,8,9-Trimethoxy-5-(4-methoxyphenyl)-1H-benzo[e][1,4]diazepin-2(3H)-one (**23a**).* Yellow solid; yield: 78%; mp: 217.8–218.9 °C; ^{1}H NMR (400 MHz, $CDCl_3$) δ 8.39 (s, 1H), 6.97 (d, J = 8.6 Hz, 2H), 6.74 (d, J = 8.6 Hz, 2H), 6.39 (s, 1H), 3.79 (d, J = 1.4 Hz, 6H), 3.71 (s, 6H), 3.41 (s, 2H).^{13}C NMR (101 MHz, $CDCl_3$) δ 171.97, 157.98, 152.33, 149.39, 140.81, 134.32, 132.33, 129.66, 121.57, 113.85, 108.86, 61.17, 60.92, 56.03, 55.26, 44.93, 37.44. HRMS (ESI) (m/z) [M + H]$^+$ calcd for $C_{19}H_{20}N_2O_5$, 357.1445; found, 357.1455. Purity: 99.0% (by HPLC).

*5-(3-Fluoro-4-methoxyphenyl)-7,8,9-trimethoxy-1H-benzo [e] [1,4]diazepin-2(3H)-one (**23b**).* White solid; yield: 75%; mp: 206.8–207.9 °C; ^{1}H NMR (400 MHz, $CDCl_3$) δ 7.83 (s, 1H), 7.40–7.35 (m, 1H), 7.32 (d, J = 9.1 Hz, 1H), 6.95 (t, J = 8.5 Hz, 1H), 6.54 (s, 1H), 4.28 (s, 2H), 3.99 (s, 6H), 3.94 (s, 3H), 3.74 (s, 3H).^{13}C NMR (101 MHz, $CDCl_3$) δ 170.79, 168.36, 153.06, 150.61, 149.55, 148.70, 144.15, 142.91, 132.28, 127.24, 126.14, 121.55, 117.35, 112.41, 108.02, 61.32, 61.08, 56.91, 56.23. HRMS (ESI) (m/z) [M + H]$^+$ calcd for $C_{19}H_{19}FN_2O_5$, 375.1351; found, 375.1365. Purity: 99.4% (by HPLC).

*7,8,9-Trimethoxy-5-(3-methoxyphenyl)-1H-benzo[e][1,4]diazepin-2(3H)-one (**23c**).* Yellow solid; yield: 78%; mp: 234.8–235.7 °C; ^{1}H NMR (400 MHz, $CDCl_3$) δ 7.81 (s, 1H), 7.29 (t, J = 5.1 Hz, 1H), 7.22–7.18 (m, 1H), 7.08–7.03 (m, 1H), 7.02–6.98 (m, 1H), 6.54 (s, 1H), 4.31 (s, 2H), 4.02–3.93 (m, 6H), 3.84 (d, J = 6.4 Hz, 3H), 3.71 (d, J = 6.4 Hz, 3H).^{13}C NMR (101 MHz, $CDCl_3$) δ 170.66, 169.90, 159.52, 148.62, 144.08, 142.70, 140.64, 129.05, 127.10, 122.48, 121.92, 116.49, 114.51, 108.33, 61.31, 61.09, 56.99, 56.23, 55.42. HRMS (ESI) (m/z) [M + H]$^+$ calcd for $C_{19}H_{20}N_2O_5$, 357.1445; found, 357.1435. Purity: 100% (by HPLC).

*7,8,9-Trimethoxy-5-(4-methoxy-3-(trifluoromethyl)phenyl)-1H-benzo[e][1,4]diazepin-2(3H)-one (**23d**).* Yellow solid; yield: 69%; ^{1}H NMR (400 MHz, $CDCl_3$) δ 8.09 (s, 1H), 7.87 (d, J = 2.0 Hz, 1H), 7.73 (dd, J = 8.7, 2.1 Hz, 1H), 7.01 (d, J = 8.7 Hz, 1H), 6.50 (s, 1H), 4.30 (s, 2H), 4.01 (t, J = 5.1 Hz, 6H), 3.95 (d, J = 6.7 Hz, 3H), 3.73 (d, J = 6.7 Hz, 3H).^{13}C NMR (101 MHz, $CDCl_3$) δ 170.66, 168.25, 159.06, 148.83, 144.25, 142.94, 134.76, 131.26, 128.71, 128.66, 127.33, 124.60, 121.34, 111.46, 107.82, 61.33, 61.11, 56.96, 56.25, 56.13. HRMS (ESI) (m/z) [M + H]$^+$ calcd for $C_{20}H_{19}N_2O_5F_3$, 425.1319; found, 425.1301. Purity: 100% (by HPLC).

Biology

Cell lines and culture. The human cancer cell lines (Hela, A549, Bel-7402, MCF-7, SW-480, MGC-803) used in this study were cultivated in DMEM containing 10% (v/v) heat-inactivated FBS, 100 units per mL penicillin, and 100 μg mL^{-1} streptomycin. The cells were incubated at 37 °C under a 5% CO_2 and 90% relative humidity (RH) atmosphere.

MTT assay. The anti-proliferative activity towards the human cancer cell lines and cell cytotoxicity towards human normal cells of the target compounds were examined by MTT assay. Briefly, when the cells were growing in the logarithmic phase, 5×10^3 cells per well cells were harvested and plated into the 96-well plates for 24 h, and then the cells were exposed to different concentrations of the test compounds for 48 h in three replicates. Afterward, 20 μL of 5 mg mL^{-1} MTT (Sigma) was added and incubated for another 4 h. Then, the suspension was discarded and 150 μL of DMSO was added to each well. The plates were shaken to dissolve the dark blue crystals (formazan) for 10 min, then the absorbance at 570 nm was measured using a multifunction microplate reader (Moleculardevices, Flex Station 3). All experiments were repeated at least three times. The IC_{50} values were calculated using Graph Pad Prism version 5.0.

Tubulin polymerisation assay *in vitro*. Tubulin polymerisation is followed by fluorescence enhancement due to the incorporation of a fluorescent reporter into the microtubules as polymerisation occurs. The tubulin polymerisation assay was monitored by the increase in fluorescence emission at 410 nm over a 60 min period at 37 °C (excitation wavelength is 340 nm) using a modification of the methods described by Bonne, D. *et al.*[18] Purified brain tubulin polymerisation kit was purchased from Cytoskeleton (BK110P, Denver, CO). The final buffer concentration for tubulin polymerisation contained 80.0 mM piperazine-*N*,*N*′-bis(2-ethanesulfonic acid) sequisodium salt (pH 6.9), 2.0 mM $MgCl_2$, 0.5 mM EGTA, 1 mM GTP, and 10.2% glycerol. Firstly, 5 μL of tested compounds were added in different concentrations, and then were warmed to 37 °C for 1 min. The reaction was initiated by the addition of 55 μL of the tubulin reaction mix.

Immunofluorescence microscopy. Hela cells were cultured in a confocal culture-dish at 3×10^4 cells per dish and cultured for 24 h. The tested compound **4a** was added at the indicated concentrations for another 24 h. Then the cells were briefly washed with PBS, and fixed with 4% pre-warmed (37 °C) paraformaldehyde for 15 min. Then cells were permeabilized with 0.5% Triton X-100 for 15 min and blocked for 30 min in 10% goat serum. FITC-conjugated mouse anti-tubulin antibody (Sigma) was added and incubated at 4 °C overnight. Cells were washed with PBS three times and incubated with goat anti-mouse IgG/Alexa-Fluor 488 (Invitrogen, USA) for 1 h. The nuclei of cells were labelled with Hochest 33342 (Sigma) in darkness at room temperature for 30 min. After washing, 1 mL

PBS was added and the samples were immediately visualized on a Zeiss LSM 570 laser scanning confocal microscope.

Molecular docking study. In our study, the X-ray structure of tubulin in complex with DAMA-colchicine (PDB code 1SA0)[24] was applied (from the RCSB Protein Data Bank (http://www.rcsb.org/pdb)) as receptor model for the docking procedure using the MOE2012 software. The colchicine binding site on the α,β-tubulin was defined as the site of ligand binding over α,β-tubulin.[26,27] Structure files of the ligand were prepared for molecular docking by defining the number of torsion angles and addition of hydrogen atoms. To validate the use of the MOE program, the docking studies were performed on the reference compound colchicine. MOE successfully reproduced the binding conformations reported in the X-ray structure with acceptable root-mean-square deviation (rmsd < 1 Å) of the atom coordinates. All structural images were prepared using PyMOL.

Cell cycle analysis. For flow cytometric analysis of DNA content, Hela cells were plated in 6-well plates (3 × 105 cells per well) and incubated in the presence or absence of compound **4a** at the indicated concentrations for 48 h. Then, the cells were harvested and fixed with ice-cold 70% ethanol overnight. Ethanol was removed by centrifugation, and the cells were washed with cold 10% phosphate buffer solution (PBS), then, treated with RNAse A (100 μg mL^{-1}, Beyotime) at 37 °C for 30 min and DNA staining solution PI (Sigma) at 4 °C for 15 min. The DNA contents of 10 000 events were measured by a flow cytometer (Beckman Coulter, Epics XL) at 488 nm. The data regarding the number of cells in different phases of the cell cycle were analyzed by EXPO32 ADC analysis software.

Apoptosis analysis. Hela cells were plated in 6-well plates (3×10^5 cells per well) and incubated in the presence or absence of compound **4a** at the indicated concentrations for 48 h to induce cell apoptosis; 0.1% DMSO was used as a vehicle control. The percentages of apoptotic cells were estimated by staining with Annexin-V-FITC and PI (Annexin-V-FITC Apoptosis Detection Kit, Beyotime) according to the manufacturer's instructions with moderate modification. After the cells were induced for 48 h, both treated and untreated cells were harvested and incubated with 5 μL of Annexin-V-FITC in binding buffer (10 mM HEPES, 140 mM NaCl, and 2.5 mM $CaCl_2$ at pH 7.4) at room temperature for 15 min. PI was then added dropwise to the medium at cold temperature, and the mixture was incubated for 10 min. Almost 10 000 events were collected for each sample and were analyzed by flow cytometry (Beckman Coulter, Epics XL). The percentage of cells undergoing apoptosis was calculated using EXPO32 ADC analysis software.

Metabolic stability study. Rat liver microsomes were prepared as previously described with slight modifications.[28,29] Fresh rat liver was homogenized in freshly prepared sucrose solution (pH 7.4) consisting of 0.25 M sucrose, 10 mM Tris–HCl, 1 mmol L^{-1} EDTA, and centrifuged at 16 000*g* for 30 min at 4 °C. The supernatant was then centrifuged at 10 000*g* for 60 min at 4 °C. The supernatant, which contained the soluble microsomes, was carefully decanted and stored at −80 °C until use. Compounds **4a** and **CA-4** at a final concentration of 50 μM were incubated in the Tris–HCl buffer containing NADPH regenerative system which consists of 1.3 mM β-$NADPNa_2$, 3.3 mM glucose 6-phosphate, 0.4 units per mL glucose 6-phosphate dehydrogenase, and 3.3 mM $MgCl_2$. Then, 1 mg mL^{-1} of rat liver microsomes were added. The samples were shaken for 60 min at 37 °C in a water bath and the incubation was stopped by adding 0.5 mL of the ice-cold acetonitrile. After centrifugation at 12 500*g* for 10 min, the supernatant was then directly analyzed by HPLC. The control group was lacking the NADPH regenerative system or the microsomes.

Conclusions

In summary, on the basis of our previous work reporting *ortho*-(3,4,5-trimethoxybenzoyl)-acetanilides and cyclic **CA-4** analogues as anti-tumour agents, in order to investigate the detailed SARs, we designed and synthesized a series of cyclic compounds as **CA-4** analogues and evaluated their anti-proliferative activity. Three aspects of the SARs which included the effect of the B-ring (hexa-cyclic or hepta-cyclic), the pattern of ring condensation (A–B ring condensation or B–C ring condensation), and C=C or C=N bond in the B ring were studied. In detail, for the hexa-cyclic compounds, A–B ring condensation is not favourable over B–C ring condensation, which was the same for the hepta-cyclic compounds. From the *in vitro* cytotoxicity results, we summarized the following three items that the hepta-cyclic structure in the B-ring, B–C ring condensation and the C=C bond in the B ring were crucial for the anti-proliferative activity.

The mechanism studies including cell cycle analysis, tubulin polymerisation inhibition assay, immunofluorescence assay, molecular docking study, and apoptosis analysis further validated that compound **4a** could effectively inhibit tubulin polymerisation, target the tubulin–microtubule system by binding to the colchicine binding site, interfere with cell mitosis, resulting in a prolonged G_2/M cell cycle arrest and ultimately lead to cell apoptosis of cancer cells. In conclusion, our work revealed a new attractive scaffold for mitosis-targeting drug discovery. As a promising new tubulin binding agent, compound **4a** is worthy of further *in vivo* antitumor evaluation as a potential chemotherapeutic agent. Further *in vitro* and *in vivo* study of compounds with B–C ring condensation, bearing C=C and hepta-cyclic structure in B ring as anti-tumour agents is also in progress.

Acknowledgements

We thank the National Natural Science Foundation of China (No. 21302235, 20972198), Guangdong Natural Science Foundation (2014A030313124) and the Fundamental Research Funds for the Central Universities (15ykpy04) for financial support of this study.

Notes and references

1 F. Pellegrini and D. R. Budman, *Cancer Invest.*, 2005, **23**, 264–273.
2 M. Kavallaris, *Nat. Rev. Cancer*, 2010, **10**, 194–204.

3 M. A. Jordan and L. Wilson, *Nat. Rev. Cancer*, 2004, **4**, 253–265.
4 G. R. Pettit, G. M. Cragg, D. L. Herald, J. M. Schmidt and P. Lohavanijaya, *Can. J. Chem.*, 1982, **60**, 1374–1376.
5 G. J. S. Rustin, S. M. Galbraith, H. Anderson, M. Stratford, L. K. Folkes, L. Sena, L. Gumbrell and P. M. Price, *J. Clin. Oncol.*, 2003, **21**, 2815–2822.
6 G. J. Rustin, G. Shreeves, P. D. Nathan, A. Gaya, T. S. Ganesan, D. Wang, J. Boxall, L. Poupard, D. J. Chaplin, M. R. L. Stratford, J. Balkissoon and M. Zweifel, *Br. J. Cancer*, 2010, **102**, 1355–1360.
7 D. W. C. Siemann, D. J. Chaplin and P. A. Walicke, *Expert Opin. Invest. Drugs*, 2009, **18**, 189–197.
8 M. Cushman, D. Nagarathnam, D. Gopal, A. K. Chakraborti, C. M. Lin and E. Hamel, *J. Med. Chem.*, 1991, **34**, 2579–2588.
9 G. R. Pettit, B. E. Toki, D. L. Herald, M. R. Boyd, E. Hamel, R. K. Pettit and J. C. Chapuis, *J. Med. Chem.*, 1999, **42**, 1459–1465.
10 H. Chen, Y. Li, C. Sheng, Z. Lv, G. Dong, T. Wang, J. Liu, M. Zhang, L. Li, T. Zhang, D. Geng, C. Niu and K. Li, *J. Med. Chem.*, 2013, **56**, 685–699.
11 Y. Z. J. Shan, Z. Liu, M. Wang and Y. Dong, *Curr. Med. Chem.*, 2011, **18**, 523–538.
12 R. Kaur, G. Kaur, R. K. Gill, R. Soni and J. Bariwal, *Eur. J. Med. Chem.*, 2014, **87**, 89–124.
13 B. L. Flynn, G. S. Gill, D. W. Grobelny, J. H. Chaplin, D. Paul, A. F. Leske, T. C. Lavranos, D. K. Chalmers, S. A. Charman, E. Kostewicz, D. M. Shackleford, J. Morizzi, E. Hamel, M. K. Jung and G. Kremmidiotis, *J. Med. Chem.*, 2011, **54**, 6014–6027.
14 A. Brancale and R. Silvestri, *Med. Res. Rev.*, 2007, **27**, 209–238.
15 Y. Wu, B. Li, F. Mao, X. Li and F. Y. Kwong, *Org. Lett.*, 2011, **13**, 3258–3261.
16 J. Sheng, F. Mao, J. Yan, L. Huang and X. Li, *RSC Adv.*, 2014, **4**, 41510–41520.
17 J. Yan, Y. Pang, J. Sheng, Y. Wang, J. Chen, J. Hu, L. Huang and X. Li, *Biochem. Pharmacol.*, 2015, **97**, 51–61.
18 D. Bonne, C. Heuséle, C. Simon and D. Pantaloni, *J. Biol. Chem.*, 1985, **260**, 2819–2825.
19 J. F. A. Diaz and J. Manuel, *Biochemistry*, 1993, **32**, 2747–2755.
20 F. G. Mollinedo and C. Gajate, *Apoptosis*, 2003, **8**, 413–450.
21 C. E. Walczak, *Curr. Opin. Cell Biol.*, 2000, **12**, 52–56.
22 P. R. A. Clarke and L. A. Allan, *Trends Cell Biol.*, 2009, **19**, 89–98.
23 F. Zhou, X. L. Han and X. Y. Lu, *Tetrahedron Lett.*, 2011, **52**, 4681–4685.
24 V. R. Choudhary and D. K. Dumbre, *Catal. Commun.*, 2011, **12**, 1351–1356.
25 F. Szabo, D. Simko and Z. Novak, *RSC Adv.*, 2014, **4**, 3883–3886.
26 F. Szabó, J. Daru, D. Simkó, T. Z. Nagy, A. Stirling and Z. Novák, *Adv. Synth. Catal.*, 2013, **355**, 685–691.
27 R. B. G. Ravelli, B. Gigant, P. A. Curmi, I. Jourdain, S. Lachkar, A. Sobel and M. Knossow, *Nature*, 2004, **428**, 198–202.
28 A. Brunschweiger, J. Iqbal, F. Umbach, A. B. Scheiff, M. N. Munkonda, J. Sévigny, A. F. Knowles and C. E. Müller, *J. Med. Chem.*, 2008, **51**, 4518–4528.
29 L. Yan and C. E. Müller, *J. Med. Chem.*, 2004, **47**, 1031–1043.